Available online at www.sciencedirect.com
SCIENCE DIRECT
Biochimica et Biophysica Acta 1665 (2004) 191–200
BIOCHIMICA ET BIOPHYSICA ACTA
BBA
http://www.elsevier.com/locate/bba

Endovesicle formation and membrane perturbation induced by polyoxyethyleneglycolalkylethers in human erythrocytes

Henry Hägerstrand[a,*], Veronika Kralj-Iglič[b,c], Miha Fošnarič[c], Malgorzata Bobrowska-Hägerstrand[a], Anna Wróbel[d], Lucyna Mrówczyńska[e], Thomas Söderström[f], Aleš Iglič[c]

[a]Department of Biology, Åbo Akademi University, Biocity, FIN-20520, Åbo/Turku, Finland
[b]Faculty of Medicine, University of Ljubljana, SI-1000, Ljubljana, Slovenia
[c]Faculty of Electrical Engineering, University of Ljubljana, SI-1000, Ljubljana, Slovenia
[d]Institute of Physics, Wroclaw University of Technology, PL-50270, Wroclaw, Poland
[e]Department of Cytology and Histology, A. Mickiewicz University, PL-61701 Poznan, Poland
[f]Turku Centre of Biotechnology, University of Turku, FIN-20520 Åbo-Turku, Finland

Received 9 September 2003; received in revised form 19 August 2004; accepted 26 August 2004
Available online 11 September 2004

Abstract

Polyoxyethyleneglycolalkylether (C_mE_n, m=12, n=8) can induce a large torocyte-like endovesicle in human erythrocytes. The present study aimed to examine how variations in the molecular structure of C_mE_n (m=10,12,14,16,18; n=1–10,23) affect the occurrence of torocyte endovesicles. Our results show that torocytes occur most frequently when m=12,14 and n=8,9. At this molecular configuration the detergents induce inward membrane bending (stomatocytic S_1–S_2 shapes) resulting in the formation of a large membrane invagination. These detergents have a strong membrane perturbing, i.e., haemolytic, effect.

Theoretical calculations indicate that a torocyte-shaped inside-out membrane vesicle can be created from a large membrane invagination due to the impact of laterally mobile anisotropic membrane inclusions. Such inclusions may be detergent–membrane component complexes or unanchored integral membrane proteins. It is shown that a nonhomogeneous lateral distribution of anisotropic membrane inclusions may stabilise the torocyte endovesicle shape, characterised by having opposite membranes in the thin central region of the vesicles separated by a certain distance. Tubular, conical or inverted conical isotropic inclusions cannot do so.

Keywords: Detergent–lipid interaction; Oxyethylene chain; Haemolysis; Cell shape; Membrane dynamic; Lipid bilayer

1. Introduction

The stomatocytogenic nonionic detergent $C_{12}E_8$ (Fig. 1) at sublytic concentrations may induce formation of a unique large torocyte-like endovesicle (torocyte) in human erythrocytes [1]. The large torocyte is different in shape from the endovesicles induced by other previously studied detergents (Fig. 2). Other stomatocytogenic detergents, such as nonionic Triton X-100 and X-114, and cationic chlorpromazine induce many small spherical endovesicles [2,3]. Our observations indicate that the torocyte is formed in a process where an initially stomatocytic pocket-like membrane invagination loses volume while maintaining a large surface area (Fig. 3). The invagination finally closes, forming a stable inside-out torocyte endovesicle having a small relative volume. The endovesicle is characterised by a large flat central area and a highly curved bulbous structure along its rim (Fig. 4). In the flat central area of the endovesicle the adjacent membranes are separated by a certain distance [1,3].

A comparison of the molecular structure of nonionic detergents that alter erythrocyte shape indicates that the nature of both the hydrophilic and the hydrophobic part of $C_{12}E_8$ is essential for the capacity of $C_{12}E_8$ to induce

* Corresponding author. Tel.: +358 2 2154089; fax: +358 2 2154748.
E-mail address: henry.hagerstrand@abo.fi (H. Hägerstrand).

0005-2736/$ - see front matter © 2004 Elsevier B.V. All rights reserved.
doi:10.1016/j.bbamem.2004.08.010

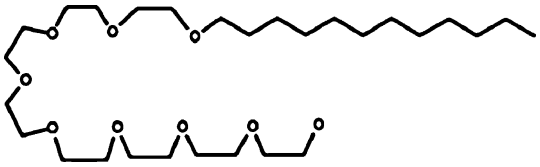

Fig. 1. Chemical structure of $C_{12}E_8$.

torocytes [1]. The present study aimed to examine how variations in the molecular structure of C_mE_n (where m is the number of carbons in the alkyl chain and n is the number of oxyethylene units) affect torocyte formation. To this purpose we studied the capacity of two detergent series, i.e., $C_{12}E_n$ (n=1–10,23) and C_mE_8 (m=10,12,14,16,18), to induce torocytes. The relation between the torocyte-forming capacity of the detergents and their capacity to induce haemolysis, shape alterations and phosphatidylserine (PS) exposure was also investigated.

In order to understand better the stability and the mechanism of formation of a torocyte endovesicle originating from one large membrane invagination, the coupling between the lateral distribution of membrane components and the vesicle shape was studied theoretically.

This study increases our knowledge of the membrane interactions of widely used polyoxyethylene detergents. It indicates the importance of in-plane orientation ordering and the nonhomogeneous lateral distribution of membrane components (inclusions) in their effect on membrane curvature and curvature-dependent vesiculation processes in biological systems.

2. Materials and methods

2.1. Chemicals

C_mE_n detergents were purchased from Fluka (Buchs, Switzerland), except $C_{12}E_{10}$ and Brij 35 ($C_{12}E_{23}$) which were, like FITC-dextran (FD-70S) and ATP kit (366-A), purchased from Sigma (St. Louis, USA). Decylglucopyranoside was purchased from Calbiochem (La Jolla, USA).

2.2. Isolation of erythrocytes

Blood was drawn from the authors (H.H., M.B.-H., A.W., L.M.) by venipuncture into heparinized tubes. The erythrocytes were washed three times in a buffer containing 10 mM HEPES, 145 mM NaCl, 5 mM KCl (pH 7.4) and subsequently suspended in the buffer at a cell density of 1.65×10^9 cells/ml. Experiments were performed within 24 h of blood sampling.

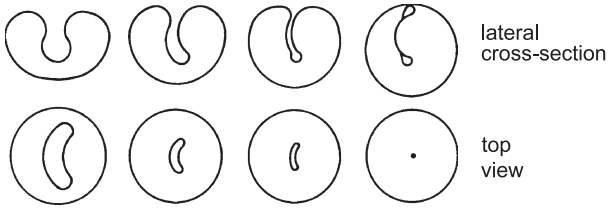

Fig. 3. Schematic figure illustrating the proposed mechanism of formation of a inside-out torocyte endovesicle in an erythrocyte. The erythrocyte is viewed as a lateral cross section and from above (top view).

2.3. Incubation with detergents

Aliquots of erythrocyte stock suspension were pipetted into Eppendorf tubes containing tempered buffer with or without detergent. The final cell density was 1.65×10^8 cells/ml (~1.5% hematocrit). Incubation was carried out under gentle mixing.

2.4. Haemolysis

Concentration-dependent haemolysis was studied by monitoring haemoglobin in the supernatants. "Haemolysis start" is defined as the concentration giving 5% haemolysis.

2.5. Shape alterations

The morphology of unfixed erythrocytes was studied in a hanging drop by phase contrast microscopy at 24 °C. Erythrocyte shape was classified according to Ref. [4].

2.6. Fluorescence microscopy (FLM)

After incubation with detergent in the presence of FITC-dextran (10 mg/ml), cells were washed three times. A drop of the sample was applied on a coverslip and covered with an object glass. The percentage of cells in a population carrying torocyte endovesicles was approximated by counting several sample fields. Samples from at least three

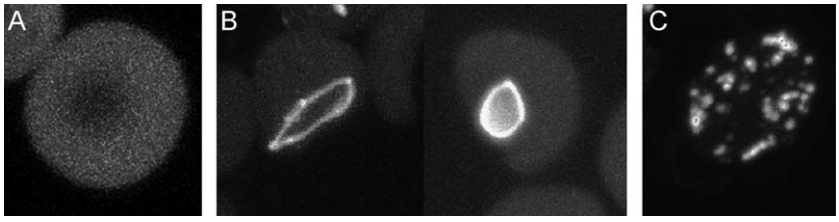

Fig. 2. Confocal laser scanning microscopy images showing human erythrocytes incubated (60 min, 37 °C) with amphiphiles in the presence of FITC-dextran (10 mg/ml). Images have an approximately similar magnification. (A) Control. (B) Two erythrocytes treated with $C_{12}E_8$ (44 μM); toroidal endovesicles. (C) Erythrocyte treated with chlorpromazine (100 μM); small spherical endovesicles. Figure partly adapted from Ref. [1].

Fig. 4. Schematic figure illustrating the principal shape of the experimentally observed C_mE_n-induced torocyte endovesicles. Note that adjacent membranes in the thin central region of the torocyte endovesicles are separated by a certain distance.

separate experiments were studied. Erythrocytes were usually studied unfixed.

2.7. Phosphatidylserine exposure

PS exposure was monitored as previously described [5]. In short, after pretreatment of erythrocytes with the aminophospholipid translocase inhibitor *N*-ethylmaleimide (10 mM, 24 °C, 30 min, two washes) and detergent-treatment (60 min, 37 °C), 1-μl Annexin-V–FITC solution (Nexins Research BV) was added to 100 μl of experimental sample (3.8 mM Ca^{2+}) and the sample incubated for 10 min on ice. The sample was then suspended in 400-μl buffer and cells (10^4 cells/sample) were analyzed for fluorescence intensity with a FACScan flow cytometer (Becton Dickinson).

3. Experimental results

3.1. Haemolysis

Since we wanted to study the effects of detergents at sublytic concentrations, the concentrations at which detergents start to induce haemolysis (5% release of haemoglobin after 60 min incubation at 37 °C and 24 °C) were initially determined (Table 1). In the $C_{12}E_n$ series, n=7,8 showed the strongest haemolytic activity, i.e., induced haemolysis at the lowest concentration. A marked decline in haemolytic activity was observed in detergents with $n \leq 4$. $C_{12}E_{23}$ did not show haemolytic activity. In the C_mE_8 series, varying in alkyl chain length, m=14,16,18 showed the strongest haemolytic activity. A strong decline in haemolytic activity occurred when m<12, i.e., with m=10. At 37 °C haemolysis occurred at slightly lower concentrations than at 24 °C. At 4 °C haemolysis occurred at about similar concentrations as at 24 °C (data not shown).

Table 1
Detergent-induced torocyte formation, hemolysis, shape alterations, phosphatidylserine (PS) exposure and membrane binding

Compound	%Erythrocytes with torocytes at conc. $C_H/2$[a]	Concentration for haemolysis start [μM]	Cell shape at conc. $C_H/2$[b]	%PS positive cells at conc. $C_H/2$[c]	K_b [$\times 10^3$ M^{-1}]
Control	0	–	D–E_2 (D–E_2/D–E_2)	0	
$C_{12}E_n$					
$C_{12}E_1$	–	~20000[d]	E_2–E_3		
$C_{12}E_2$	0	~4000 (~4000)[d]	E_2–E_3 (E_2–E_3/E_2–E_3)		
$C_{12}E_3$	0	276 (410)	D (E_1/E_2–E_3)		
$C_{12}E_4$	0	141 (190)	D (E_1/E_2–E_3)	40	
$C_{12}E_5$	0	95[e] (125)	S_1[e] (S_1/E_2–E_3)		
$C_{12}E_6$	1–3	86 (100)	S_2–S_1 (S_1/D)	28	
$C_{12}E_7$	3–8	69 (90)	S_2 (S_2–S_1/D)		
$C_{12}E_8$	5–20	69[e] (95)	S_2[e] (S_1/D)	30	
$C_{12}E_9$	8–20	81 (110)	S_2–S_1 (S_1/D)		
$C_{12}E_{10}$	1–5	105 (~135)	S_2–S_1 (S_1/E_1–E_3)	40	
$C_{12}E_{23}$	0–2	[f] ([f])	S_1–D (S_1–D/D–E_3)[g]	<5	
C_mE_8					
$C_{10}E_8$	3–9	430[e] (800)	SS–S_2[e] (S_2/S_2)	52	2.4[h], 0.2[i]
$C_{12}E_8$	5–20	69[e] (95)	S_2[e] (S_2/S_1–D)	28	6.0[h], 10.6[i]
$C_{14}E_8$	10–17	45[e] (50)	S_2–S_1[e] (S_1–D/D)	24	25.5[h]
$C_{16}E_8$	1–4	49[e] (55)	S_1[e] (S_1–D/E_1–E_2)	16	31.5[h]
$C_{18}E_8$	0–2	54[e] (55)	S_1–D (S_1–D/E_1–E_2)	12	47.7[h]

Erythrocytes were incubated with detergent for 60 min at 37 °C. Results for experiments performed at 24° and 24°/4 °C are given in parentheses.
Haemolysis start=detergent concentration inducing 5% release of haemoglobin. Data are the average of two to four experiments.
$C_H/2$=50% of the amphiphile concentration inducing haemolysis start.

[a] Data are the range of values found in two to six experiments.

[b] Predominant shapes were classified according to Ref. [4]. D=discocyte, S_1=stomatocyte type 1, S_2=stomatocyte type 2, SS=sphero-stomatocyte, E_1=echinocyte type 1, E_2=echinocyte type 2, SE=sphero-echinocyte. Data are based on three or more experiments.

[c] Results from one representative experiment out of four is shown.

[d] The system may not be well equilibrated due to solubility problems.

[e] Data in line with those previously reported [44].

[f] No haemolytic effect.

[g] Shape at 10 mM.

[h] Membrane binding constants (K_b) are from Ref. [20]. K_b for Triton X-100 was 5.9 ($\times 10^3$ M^{-1}).

[i] From Ref. [21], assuming a lipid partial volume of 0.658 L/mol.

3.2. Shape alterations

Since it was thought that the torocyte is formed from a large membrane invagination created in a stomatocytogenic process, the shape altering characteristics of detergents were investigated. The shape alterations induced by detergents at concentrations 50% of those inducing the start of haemolysis after 60-min incubation ($C_H/2$) at different temperatures are shown in Table 1. In the $C_{12}E_n$ series, the induced shape alterations at 37 °C varied with n from a slightly echinocytogenic effect (n=1,2), through no significant shape perturbation (n=3,4), to a significant stomatocytogenic effect (n=5–10), and back to a weak stomatocytogenic effect (n=23). $C_{12}E_n$ (n=7,8) showed the strongest stomatocytogenic effect. At 24 °C less stomatocytic shapes occurred with all detergents. No stomatocytic shapes occurred at 4 °C. In the C_mE_8 series, the strongest stomatocytogenic effect at all temperatures was seen with m=10. The stomatocytogenic activity declined with alkyl chain length. Notably, with $C_{10}E_8$ marked stomatocytosis also occurred at 4 °C. With all detergents qualitatively similar types of shape alterations were also seen at concentrations 25% and 75% of those inducing the start of haemolysis (not shown). For comparison, we also tested the nonionic detergent poly(oxyethylene)20-sorbitane-monolaurate (Tween 20), which bears about 20 oxyethylene units distributed around a bulky polar head. Tween 20, which induces haemolysis at ~8 mM, was stomatocytogenic at ~0.8 mM (not shown).

3.3. Torocyte formation

The percentage of erythrocytes containing a torocyte after incubation with detergent for 60 min at 37 °C at $C_H/2$ is shown in Table 1. For comparison, data on haemolysis, shape alterations and phosphatidylserine exposure at 37 °C are included. A torocyte occurred most frequently in erythrocytes treated with $C_{12}E_n$ (n=9,8) and C_mE_8 (m=14,12). There was usually one torocyte structure in the cell. No or very few torocytes were formed by $C_{12}E_n$ (n=2,3,4,5,23) and $C_{18}E_8$. No torocytes occurred in untreated erythrocytes (control). The abundance of torocytes increased with incubation time from 60 to 120 min by 50–100% (data not shown). Further increase of incubation time did not affect the abundance of torocytes. At incubations shorter than 30 min only a few torocytes were observed. The abundance of torocytes increased with surfactant concentration. At a low concentration, i.e., 25% of that at which haemolysis starts, only a few torocyte endovesicles were observed, while a largely similar number of torocytes was found at concentrations 50% and 75% of haemolysis start concentrations. The abundance of torocytes decreased with lowering of temperature (data not shown). At 24 °C torocyte endovesicles were found in erythrocytes treated with detergents $C_{12}E_n$ (n=7–10) and C_mE_8 (m=10,12). No torocytes were seen in samples incubated at 4 °C. The relation between the energy status of erythrocytes and the formation of torocytes was investigated. Supplementation of the buffer with orthovanadate (5 mM), sodium fluoride (10 mM), *N*-ethylmaleimide (10 mM) or glucose (10 mM, see also Refs. [1,3]), treatments supposed to alter the energy status of erythrocytes, did not markedly affect the abundance of detergent-induced torocytes. Erythrocytes stored 3 days without glucose (4 °C) had the capacity to form torocytes. The ATP level in erythrocytes was lowered by treatment (60 min, 37 °C) with $C_{12}E_8$ (37±6%, n=6) and chlorpromazine (27±7%, n=4) at concentrations where endovesiculation is induced. The ATP depletion induced by $C_{12}E_8$ is in line with its strong potency to induce PS exposure in the human erythrocyte [5]. ATP may be consumed for inward transport of PS. Torocyte formation is not due to the presence of remnant white blood cells (data not shown). It readily occurred following filtration [6] of blood stock through a micro- and α-cellulose column. Torocytes survived subsequent induction of echinocytosis induced when cells made contact with glass between slides and coverslips. Thus, after their formation torocytes seem to be independent of the overall erythrocyte shape. The reason for the rather low abundance of torocyte-bearing cells even in samples treated with the most efficient detergent species remains unclear. We could find no difference in the capacity of erythrocytes from different fractions of an "age-fractionated" [7] erythrocyte suspension to form torocytes (data not shown).

3.4. Annexin-V–FITC binding

To study whether the transmembrane phospholipid redistribution, i.e., PS exposure, is related to the torocyte-forming capacity of the detergents, detergents were tested for their capacity to induce Annexin-V–FITC binding (PS exposure) at $C_H/2$ (60 min, 37 °C) (Table 1). The percentage of erythrocytes that bound Annexin-V–FITC above the control level was monitored. The number of Annexin-V–FITC positive cells was smaller with $C_{12}E_n$ (n=6,8) than with (n=4,10). Few positive cells occurred with (n=23). In the C_mE_8 series a decline in Annexin-V–FITC binding with an increase in m occurred. Decylglucopyranoside was included in this study since it is a nonionic detergent that does not induce torocytes. The Annexin-V–FITC binding of decylglucopyranoside was similar to that of $C_{12}E_8$.

4. Discussion

4.1. The effect of oxyethylene and carbon chain length on membrane perturbation

The length of the hydrophilic oxyethylene chain strongly influenced the capacity of $C_{12}E_n$ to form torocytes, being most potent when n=8,9 (Table 1). The torocyte-forming potency of detergents ($C_{12}E_{1–23}$) corre-

lated positively with their haemolytic potency, and partly with their stomatocytogenic (membrane inward bending) effect, the most effective torocyte formers inducing S_1–S_2 shapes. Concerning the membrane perturbing effect of C_mE_n detergents, it has previously been reported that $C_{12}E_n$ where n<3 poorly expands the surface of a palmitoyloleoylphosphatidylcholine (POPC) monolayer, while the expansion increases with n from n=4 to n=8 [8]. These results were taken to indicate that the effective molecular shape of C_mE_n becomes more cone-shaped (large hydrophilic head group/small hydrophobic group) with an increase in oxyethylene chain length (n). The increase in molecular up–down asymmetry with the oxyethylene chain length may be due to a coiled conformation of the oxyethylene chain (see Appendix A). In accordance with monolayer studies, $C_{12}E_n$ detergents with n<3 are thought to fit into a lipid bilayer without a markedly disturbing effect due to their small head groups which hardly expand the bilayer head group region [9,10]. The effective molecular shape of these detergents has been characterised as tubular (n=2,3) or even inverted cone shaped (n=1). On the other hand, $C_{12}E_n$ (n>4) appear to have a more conical shape than the membrane lipids, leading to a marked destabilisation of the membrane [9–11]. It can be suggested that besides a conical shape, a probable in-plane shape polarity of the head group of C_mE_n detergents may additionally increase the membrane perturbing effect. The above reported results from model membrane studies are in agreement with the results of the present study. The weak potency of $C_{12}E_n$-detergents with only a few oxyethylene units to induce haemolysis is apparently due to less effective membrane perturbation. Concerning erythrocyte shape alterations, it should be noted that these are not primarily due to detergent-induced bending in one membrane leaflet of the cell [12], but rather to an asymmetric distribution of the detergent between the bilayer leaflets [13]. Torocyte-forming detergents induce stomatocytosis and should therefore be preferentially accumulated in the inner membrane leaflet of the cell. The mechanism behind the stomatocytogenic effect of C_mE_n detergents is discussed in Appendix A. When it comes to $C_{12}E_n$ with a longer oxyethylene chain (n>8), increased hydrophilicity may hinder a deep membrane penetration (and flip). Accordingly, it was observed that $C_{12}E_n$ (n=10) was less effective in inducing haemolysis, stomatocytosis and torocytes compared to detergents with a slightly shorter oxyethylene chain. Our results are in accordance with those of Refs. [14,15], showing that polyoxyethylene detergents with oxyethylene chain length (n=7–13) are haemolytic, while those with a shorter (n=4,5) and longer chain (n=20) are not. Detergents with an oxyethylene chain of medium length (n=10) were accordingly shown to increase the cation permeability in erythrocytes more than those with a short (n=4) or long (n=20) oxyethylene chain [16]. Unfortunately, data on $C_{12}E_n$ binding to the erythrocyte membrane is still lacking. However, studies on $C_{12}E_n$ partition into model membranes have shown that the POPC vesicle/water partition decreases from $C_{12}E_2$ to $C_{12}E_8$ [17,18]. This is probably due to the increased hydrophilicity of the oxyethylene chain with increase in n. Since a largely similar qualitative relative binding of detergents to erythrocytes and phospholipid vesicles has been indicated [19], these results suggest that binding and membrane perturbation of $C_{12}E_n$ (n=2–8) correlate negatively.

The length of the hydrophobic carbon chain also influenced the capacity of C_mE_8 to form torocytes, C_mE_8 (m=14,12) being the most effective (Table 1). The torocyte-forming potency did not correlate positively in a simple direct way with the degree of stomatocytosis. $C_{10}E_8$ induced more pronounced stomatocytic shapes (sphero-stomatocytes) than the other C_mE_8 detergents, but the number of torocytes was smaller than with C_mE_8 (m=14,12). Electron microscopic studies showed abundant formation of not torocytic but small spherical endovesicles in $C_{10}E_8$-treated cells (not shown). Thus, too strong an inward membrane bending, leading to formation of small highly curved endovesicles, apparently is not favourable for torocyte formation. Similarly, too weak a stomatocytic shape transformation (C_mE_8, m=16,18) is also not beneficial for torocyte formation. The conclusion is that a stomatocytic S_1–S_2-like shape, involving formation of one large invagination, is the most favourable one for torocytes to be formed. The counteracting effects of membrane bending and binding may give, at the concentration used, an S_1–S_2 cell shape with C_mE_8 (m=14,12). Notably, detergents with a strong torocyte-forming potency are highly haemolytic. For C_mE_8, binding to the erythrocyte membrane increases with alkyl chain length (hydrophobicity) [20,21] (Table 1). Similarly, data from model membrane studies show that the POPC/water partition increases in the order $C_{10}E_7$<$C_{12}E_7$<$C_{14}E_7$ [18]. The haemolytic potency of C_mE_8 detergents may thus be related to the counter-directional effects of binding and impact on intrinsic curvature, giving an optimum around (m=14) at 37 °C. For C_mE_8 detergents, there is a negative correlation between binding and phosphatidylserine exposure. It can be suggested that detergents with a long alkyl chain bind strongly due to deep penetration of the alkyl chain into the hydrophobic portion of the lipid bilayer. At low concentrations such deep penetration may result in small bending (perturbation) of the membrane leaflet. On the other hand, detergents with a shorter chain may induce a stronger imbalance in the leaflet due to less deep penetration into the hydrophobic region.

To summarise, the torocyte-forming potency of detergents appears to depend primarily on an appropriate shape (S_1–S_2) altering effect, and secondarily on a strong membrane perturbing (haemolytic) potency. As is discussed below, a strong membrane perturbation may give rise to formation and lateral redistribution of membrane inclusions, which may be necessary to give the membrane invagination a torocyte shape.

4.2. The possible role of membrane inclusions in the formation of torocyte vesicles

Within the standard bending elasticity models of the bilayer membrane [22–24], the opposing membranes in the thin central region of the calculated torocyte vesicle shapes [22,25] are in close contact (Fig. 5), i.e., the resultant forces on the two membranes in contact are balanced. However, as indicated by transmission electron and confocal laser scanning microscopy, the opposite membranes in the central region of the $C_{12}E_8$-induced torocyte endovesicles are separated by a certain distance [1,3]. Based on these observations, we suggested that the observed shapes of torocyte endovesicles may not be fully explained by the standard bending elasticity models [25,26]. We have therefore studied which additional physical mechanism, besides a minimisation of the membrane bending energy, might take place in the formation of such torocyte endovesicles.

Fig. 6 shows the calculated equilibrium vesicle shapes determined by minimisation of the free energy of the membrane with anisotropic inclusions, as described in Appendix B. It can be seen in Fig. 6 that the calculated equilibrium vesicle shape resembles the observed torocyte vesicle shape, which has a thin central region with the opposite membranes separated by a certain distance (Figs. 2 and 4). Based on these results, we propose that coupling between the nonhomogeneous lateral distribution of anisotropic membrane inclusions and the membrane curvature may offer a possible explanation for the characteristic shape

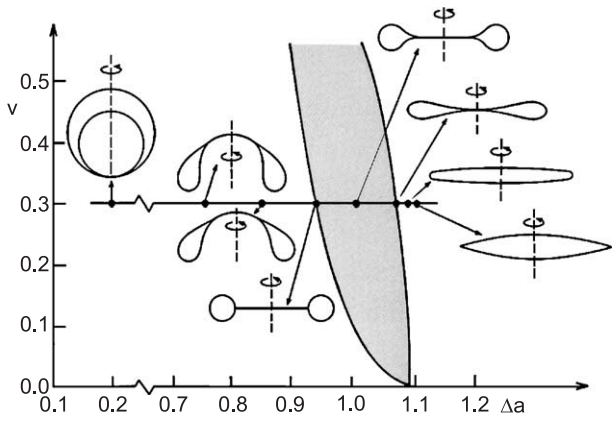

Fig. 5. Region in the v–Δa phase diagram belonging to the class of axisymmetrical torocyte vesicle shapes with equatorial mirror symmetry. The left side of the phase diagram belongs to torocyte shapes without equatorial mirror symmetry. The phase diagram shows vesicle shapes corresponding to the minimal local bending energy as a function of the relative vesicle volume (v) and of the relative difference between the areas of the two membrane lipid layers (Δa). Both of these parameters are normalized relative to the corresponding values or the spherical vesicle that has the same membrane area (adapted from Ref. [25]). Note that the predicted torocyte vesicle shapes have the opposite membranes in the thin central region of the vesicles always in close contact, i.e., there is no space between opposite membranes in the central region of the vesicles. The role of hydration forces, electric double layer repulsion and steric forces [28] in the interaction between the opposite membranes in the thin central region of the vesicles has not been considered explicitly.

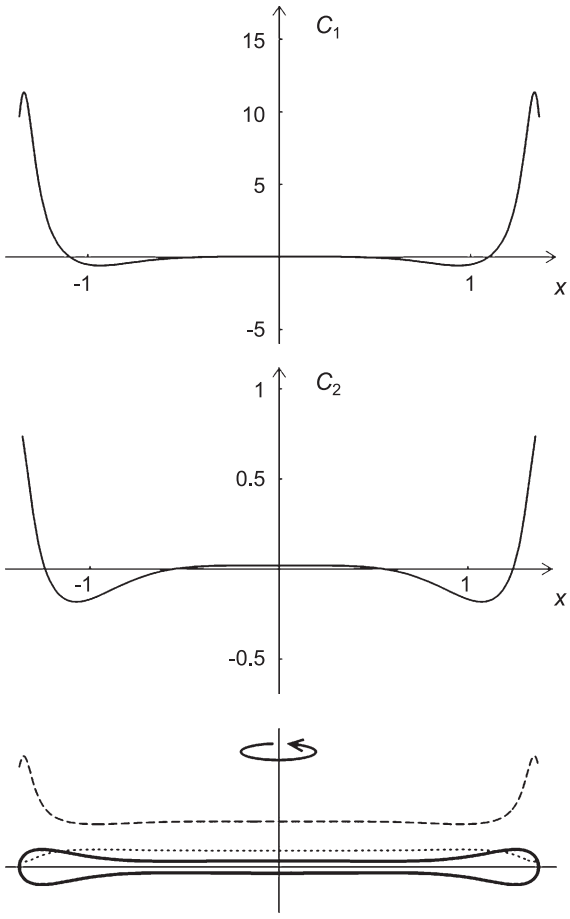

Fig. 6. The equilibrium vesicle shape and the corresponding relative area density of membrane inclusions calculated for the normalised principal curvatures of the intrinsic shape of the inclusion C_{1m}=34 and C_{2m}=0 at a relative vesicle volume of 0.16. The corresponding values of the membrane principal curvatures C_1 and C_2 are also given. The inclusions are distributed in the outer (broken line) and inner (dotted line) lipid leaflet of the inside–outside endovesicle membrane. The values of the model parameters used in calculations are: $N_o kT/8\pi k_c$=80, $N_i kT/8\pi k_c$=20, $4\pi\xi/kTA$=0.01 and $\xi^*=\xi$. The principal curvatures are normalized relative to the corresponding values for a spherical vesicle with the same membrane area [35].

of the observed torocyte vesicles with separated membranes in the flat central region of the vesicle. Tubular, conical or inverted conical isotropic membrane inclusions are unable to produce such an effect.

In the calculations of theoretical vesicle shapes (Fig. 6), it was assumed that the inclusions are located in both lipid leaflets of the inside–outside endovesicle membrane. Location of the inclusions in only one leaflet gives an essentially similar result. Fig. 6 also shows the area density of the membrane inclusions in both membrane leaflets of the vesicles. The inclusions are accumulated at the regions of favourable curvature and depleted from the regions of unfavourable curvature. The lateral distributions of the membrane inclusions in the outer and inner layers are different.

The accumulation of membrane inclusions at the regions of favourable curvature may bring the inclusions to the

distance where the interactions between the inclusions become effective [27]. Therefore, growth of the torocyte membrane may be additionally driven by direct inclusion–inclusion interactions.

The value of relative vesicle volume (v) and the value of the interaction constant (ξ), describing the strength of the interaction between the inclusion and the membrane continuum (see Appendix B), were chosen so that the calculated vesicle shape resembles the observed one as much as possible (Fig. 6). At larger relative volumes the distance between the opposing membranes in the flat central region of the calculated stable vesicle shape would be larger, while a decrease of the relative volume would lead to closer approach of the opposite membranes in the flat central region of the vesicle. If the distance between the inner surfaces of the opposing membranes would be small enough, then at very low vesicle relative volumes the long-range electric double layer repulsion [28] should be taken into account in the minimization procedure. Since the observed torocyte endovesicles are inside–outside vesicles, the membrane glycocalyx is localized on the inner surface of the vesicle. Therefore, the electric double layer on the inner side of the vesicle membrane is almost completely generated by the negative charges of sialic acids in the glycocalyx. The around 5-nm-thick layer of glycocalyx may also generate steric repulsion [28] between the opposite membranes in the thin central region of the torocyte endovesicles. The glycocalyx may diminish or abolish short-range attractive van der Waals and short-range attractive or oscillatory hydration forces between the opposing membranes, as the estimated range of these forces is not longer than 2 nm [28].

If the number of oxyethylene groups in the hydrophilic head of the C_mE_n molecule is large enough, the effective molecular shape of C_mE_n is conical [8–11] and satisfies conditions for formation of highly curved structures [11], such as small spherical micelles [29]. The intrinsic principal curvatures of C_mE_n molecules forming micelles are expected to be of the same order of magnitude as the principal curvatures of these micelles. Thus, the conical molecular shape of C_mE_n per se would favour the formation of many small spherical endovesicles having very large and equal positive principal membrane curvatures (C_1=C_2). Such endovesicles are formed by Triton X-100 and chlorpromazine [1]. It has been shown in Fig. 6 that only membrane inclusions that have an effective shape that differs substantially from the conical molecular shape favour the characteristic torocyte vesicle shape [26]. Conical isotropic membrane inclusions are unable to produce such an effect.

The suggested anisotropic membrane inclusions may be C_mE_n–lipid complexes [1] or may involve proteins unanchored by the C_mE_n-treatment. The inclusions may show similarities with supposed membrane microdomains or rafts. In fact, we recently observed that cholesterol depletion with methyl-β-cyklodextrin, under conditions that remove membrane cholesterol and lead to abolishment of raft structures [30], seemed to prevent torocyte formation (Hägerstrand et al., unpublished results). Only small spherical endovesicles were formed. The skeleton network normally restricts the lateral mobility and distribution of membrane embedded proteins (Ref. [31] and references therein). However, in C_mE_n-treated erythrocytes the skeleton–bilayer interactions could be impaired. Therefore, unanchoring and lateral redistribution of integral membrane proteins, which can in general be considered as anisotropic inclusions [32], may be a driving force in torocyte formation.

Estimation of the average inclusion radius (R_i) from the value of the interaction constant $\xi \approx 10^{-15}$ kT m^2 (Fig. 6) gives us the value $R_i \approx (\xi\lambda/3\pi k_c)^{1/3} \approx 2$ nm [33], where $\lambda \approx 1$ nm is the typical decay length of the inclusion induced membrane perturbation and $k_c \approx 10$–20 kT. The value $R_i \approx 2$ nm roughly corresponds to the area of 20 lipid molecules or to the area of the membrane protein. This is in accordance with the above assumption that the suggested anisotropic membrane inclusions are unanchored membrane proteins or C_mE_n–lipid complexes.

The proposed theoretical model for explaining the finite distance between the opposing membranes in the thin central region of the observed C_mE_n-induced torocyte vesicle shapes is in line with recent experimental results which indicate that particular membrane components in large flattened vesicles in Golgi bodies are concentrated in certain regions [34]. Thus, the finite distance in the central region of the Golgi vesicles may also be related to a nonhomogeneous lateral distribution of membrane components.

5. Conclusion

C_mE_n-induced torocyte formation in human erythrocytes apparently starts with the formation of a large pocket-like invagination in a stomatocytogenic (S_1–S_2) process. The invagination finally closes, forming the characteristic torocyte endovesicle having opposing membranes in the thin central region of the vesicle separated by a certain distance. It was shown in this work that the nonhomogeneous lateral distribution of anisotropic inclusions may be essential in forming such torocyte endovesicles. Tubular, conical or inverted conical isotropic inclusions are unable to produce such torocytes. The calculated correlation between the local membrane composition and the local membrane curvature in torocyte endovesiculation indicates the importance of a curvature-dependent sorting of membrane components and a curvature-dependent formation of membrane domains in vesiculation processes in biological systems.

When a detergent is added to the erythrocyte suspension it first interacts with an almost flat erythrocyte membrane. For an almost flat membrane the lateral redistribution of anisotropic membrane inclusions is negligible [32,35].

Therefore, we believe that the initial stage of the torocyte-forming process seems to be largely driven by the stomatocytogenic effect of C_mE_n molecules. It is only when the stomatocytic invagination approaches a flat structure with a bulky rim that the lateral redistribution of membrane inclusions becomes important.

The involvement of C_mE_n-induced anisotropic membrane inclusions in torocyte formation seems plausible. The conical molecular shape of C_mE_n per se would not favour torocyte formation, but the formation of many small spherical endovesicles [1]. Formation of membrane inclusions apparently requires a strong membrane perturbation as indicated by the haemolytic potency of the strongest torocyte formers. It can be speculated that destabilisation of phospholipid interactions and/or de-anchoring of integral membrane proteins leads to the formation of laterally mobile membrane complexes, i.e., inclusions.

Acknowledgements

We are indebted to Gunilla Henriksson for performing the venipunctures, to Esa Nummelin for help with the artwork and Sylvio May for useful discussions. We are also indebted to Svenska Kulturfonden, Oskar Öflunds Stiftelse, Ella och Georg Ehrnroths Stiftelse, and the Research Institute at the Åbo Akademi University and the Ministry of Science of Republic of Slovenia, for their financial support.

Appendix A. The stomatocytogenic effect

The relation between the molecular properties of C_mE_n and its membrane effects may probably be better understood by taking into consideration the reported charge properties of C_mE_n detergents, i.e., the polyoxyethylene chain (see Ref. [36] and references therein). In a hydrophobic environment nonionic surfactants containing polyoxyethylene (or similar) subunits may attract, apparently via dipole–ion interactions [37], cations (mono- and divalent metal cations and protons) resulting in positively charged complexes [38–41]. Cations are co-ordinated to oxygen atoms in the polyoxyethylene chain. In accordance with this, the positive charge character of the $C_{10}E_8$ polyoxyethylene chain was recently reported [42]. The capacity of the ethylene chain to bind a metal cation depends on its length, increasing markedly up to n=6–7 (Ref. [43] and references therein). This relation between the oxyethylene chain length and its capacity to bind a cation may explain the relation between erythrocyte shape alterations (and monolayer expansion) and C_mE_n oxyethylene chain length, and thereby also the hitherto unexplained stomatocytogenic effect of nonionic detergents like $C_{12}E_8$ and Triton X-100. Anticipating an increased cation-binding capacity with the length of the ethylene oxide chain, at a certain oxyethylene chain length ($n \geq 4$) the cation binding of C_mE_n is apparently strong enough to result in a slight accumulation of some C_mE_n–cation complexes in the inner membrane leaflet of the cell due to interaction with negatively charged phospholipids in this leaflet. Stomatocytosis will consequently be induced. Strong support for the view that polyoxyethylene detergents induce stomatocytosis due to their accumulation in the inner membrane leaflet of the cell after interaction with net negative phospholipids comes from experiments with field-pulse-treated erythrocytes showing that Triton X-100 did not induce stomatocytosis in phospholipid-symmetrised discocytic cells [44]. Since $C_{12}E_8$ has been shown to rapidly flip over (phospholipid) membranes [45], it can be suggested that only a fraction of the membrane intercalated $C_{12}E_8$ pool binds cations and is markedly attracted to the inner membrane leaflet of the cell. This is consistent with the slow and relatively weak stomatocytogenic effect of $C_{12}E_8$ compared to several other stomatocytogenic detergents, e.g., chlorpromazine [46]. It seems less likely that C_mE_n is predominantly accumulated in the inner membrane leaflet of the cell membrane due to interactions of the

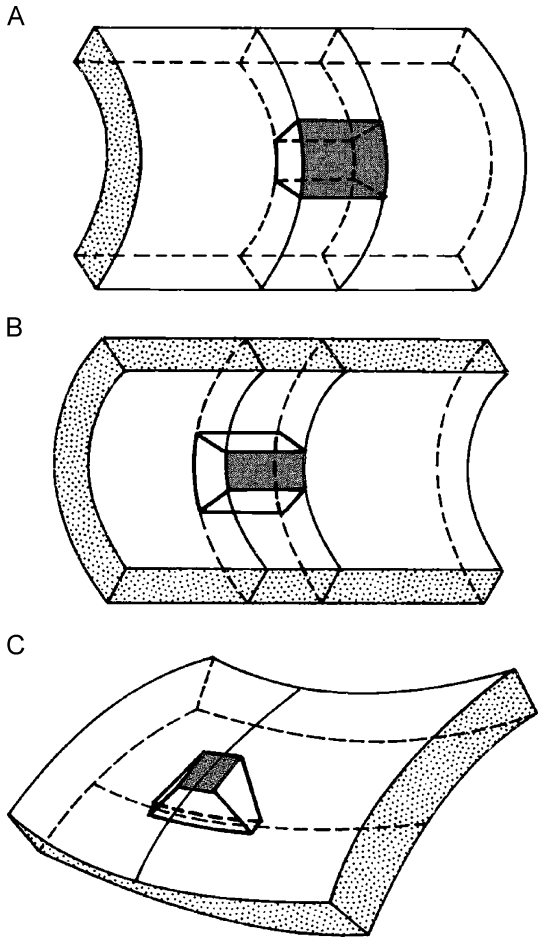

Fig. 7. Schematic figure illustrating different intrinsic shapes of the membrane inclusions characterized by the two principal curvatures, C_{1m} and C_{2m}. The hydrophilic surface of the inclusion is marked by shading. Three characteristic intrinsic shapes of inclusions are shown: (A) $C_{1m}>0$ and $C_{2m}=0$, (B) $C_{1m}<0$ and $C_{2m}=0$ and (C) $C_{1m}>0$ and $C_{2m}<0$.

oxyethylene chain directly with phospholipid head groups in this leaflet or with the membrane skeleton. Cytoskeletal proteins ordinarily do not interact with nonionic detergents [47]. Several possible membrane effects of C_mE_n remain to be studied. An involvement of detergent-stabilised transient membrane pores [33] in the transmembrane movements of C_mE_n detergents cannot be excluded. Also, it cannot be excluded that some phospholipids in the outer leaflet of the cell membrane are extracted into mixed C_mE_n–phospholipid micelles. Furthermore, a possible impact of transmembrane redistributions of phospholipids in C_mE_n-induced stomatocytic shape alterations should also be taken into account (see Ref. [48]). $C_{12}E_8$ has been shown to propagate phosphatidylserine exposure [5]. C_mE_n-induced stomatocytic shape alterations, and thereby torocyte formation, may also be affected by a possible echinocytogenic effect of ATP depletion occurring under incubation.

Appendix B. Calculation of the equilibrium inside–outside vesicle shapes with anisotropic membrane inclusions

The equilibrium shape of the inside-out torocyte vesicle corresponding to the minimal membrane free energy was determined as described in detail elsewhere [26]. To obtain the stable vesicle shape at given area (A) and volume (V), we minimised the membrane free energy, which is taken to be the sum of the local membrane bending energy [22],

$$F_b = \frac{1}{2}k_c \int (2H - C_0)^2 dA, \quad (1)$$

and the free energy contributed by the laterally mobile membrane inclusions in the outer (F_o) and in the inner (F_i) membrane leaflet of the inside–outside vesicle [32]:

$$F_j = -N_j kT \ln\left[\frac{1}{A}\int q_j I_0\left(\frac{\xi+\xi^*}{2kT}DD_m\right)dA\right],$$

$$q_j = \exp\left(-\frac{\xi}{2kT}\left(\delta_j H - H_m\right)^2 - \frac{\xi+\xi^*}{4kT}\left(D^2+D_m^2\right)\right), \quad (2)$$

where j=o, i. The index o denotes the outer leaflet and the index i denotes the inner leaflet of the vesicle membrane bilayer, δ_o=1, δ_i=−1. Here, C_1 is the maximal and C_2 is the minimal principal curvature of the membrane, C_{1m} and C_{2m} are the intrinsic principal curvatures of the inclusions (Fig. 7) describing the intrinsic shape of the inclusion [31,35], k_c is the local bending modulus, ξ and ξ^* are the constants representing the strength of the interaction between the inclusion and the membrane continuum, C_0 is the spontaneous curvature of the membrane, dA is the infinitesimal membrane area element, $D=(C_1-C_2)/2$ is the curvature deviator, $H_m=(C_{1m}-C_{2m})/2$, $D_m=(C_{1m}-C_{2m})/2$, N_j is the total number of the inclusions in the j-th leaflet of the vesicle membrane, I_0 is the modified Bessel function, k is the Boltzmann constant and T is the temperature. For the sake of simplicity, the non-local bending energy [23,24] is not considered.

If $C_{1m}=C_{2m}$, the inclusion is isotropic with respect to rotation in the plane of the membrane, while if $C_{1m}\neq C_{2m}$, the inclusion is anisotropic (Fig. 7). The two principal curvatures of the intrinsic shape of the inclusion C_{1m} and C_{2m} may also describe the up–down symmetry of the isotropic ($C_{1m}=C_{2m}$) inclusion [29], as well as the in-plane polarity of the anisotropic ($C_{1m}\neq C_{2m}$) inclusion (Fig. 7) [31,49].

In the minimisation procedure the shape of the vesicle and the lateral distribution of the inclusions are derived from the same basic assumptions [32]. Consequently, the calculated lateral distribution of the inclusions and the vesicle shape are interdependent. In this work the analysis is restricted to axisymmetric vesicle shapes parameterised by a function involving four independent parameters [26]. In the case of C_mE_n-induced torocyte vesicles the smaller principal radius of curvature (reciprocal of the principal curvature C_1) of the vesicle membrane in the peripheral region of the torocyte rim is around 100 nm, while the larger principal radius of curvature (reciprocal of the principal curvature C_2) in this region is around 10 times larger (see Fig. 2). In normalised quantities this would correspond to $C_1 \approx 10$ and $C_2 \approx 1$. In Fig. 6 the values C_{1m}=34 and C_{2m}=0 were taken into account.

References

[1] M. Bobrowska-Hägerstrand, V. Kralj-Iglič, A. Iglič, K. Bialkowska, B. Isomaa, H. Hägerstrand, Toroidal membrane endovesicles induced by polyethyleneglycol dodecylether in human erythrocytes, Biophys. J. 77 (1999) 3356–3362.

[2] H. Hägerstrand, B. Isomaa, Vesiculation induced by amphiphiles in erythrocytes, Biochim. Biophys. Acta 982 (1989) 179–186.

[3] H. Hägerstrand, B. Isomaa, Morphological characterization of exovesicles and endovesicles released from human erythrocytes after treatment with amphiphiles, Biochim. Biophys. Acta 1109 (1992) 117–126.

[4] M. Bessis, Red Cell Shapes. An illustrated classification and its rationale, in: M. Bessis, R.I. Weed, P.F. Leblond (Eds.), Red Cell Shape; Physiology, Pathology, Ultrastructure, Spinger-Verlag, Heidelberg, 1973, pp. 1–24.

[5] H. Hägerstrand, T.H. Holmström, M. Bobrowska-Hägerstrand, J.E. Eriksson, B. Isomaa, Amphiphile-induced phosphatidylserine exposure in human erythrocytes, Mol. Membr. Biol. 15 (1998) 89–95.

[6] E. Beutler, C. West, K.G. Blume, The removal of leukocytes and platelets from whole blood, J. Lab. Clin. Med. 88 (1976) 328–333.

[7] H.U. Lutz, P. Stammler, S. Fasler, M. Ingold, J. Fehr, Density separation of human red blood cells on self-forming Percoll gradients: correlation with cell age, Biochim. Biophys. Acta 1116 (1992) 1–10.

[8] G. Lantzsch, H. Binder, H. Heerklotz, M. Wendling, G. Klose, Surface areas and packing constraints in POPC/C12EOn membranes. A time-resolved fluorescence study, Biophys. Chemist. 58 (1996) 289–302.

[9] H. Heerklotz, H. Binder, G. Lantzsch, G. Klose, A. Blume, Lipid/detergent interaction thermodynamics as a function of molecular shape, J. Phys. Chem., B 101 (1997) 639–645.

[10] H. Heerklotz, H. Binder, H. Schmiedel, Excess enthalpies of mixing in phospholipid-additive membranes, J. Phys. Chem., B 102 (1998) 5363–5368.
[11] D. Otten, L. Lobbecke, K. Beyer, Stages of the bilayer–micelle transition in the system phosphatidylcholine-C12E8 as studied by deuterium and phosphorus NMR, light scattering, and calorimetry, Biophys. J. 68 (1995) 584–597.
[12] F.A. Kuypers, B. Roelofsen, W. Berendsen, J.A. Op den Kamp, L.L. van Deenen, Shape changes in human erythrocytes induced by replacement of the native phosphatidylcholine with species containing various fatty acids, J. Cell Biol. 99 (1984) 2260–2267.
[13] M.P. Sheetz, S.J. Singer, Biological membranes as bilayer couples. A molecular mechanism of drug–erythrocyte interactions, Proc. Natl. Acad. Sci. 71 (1974) 4457–4461.
[14] D. Trägner, A. Csordas, Biphasic interaction of Triton detergents with the erythrocyte membrane, Biochem. J. 244 (1987) 605–609.
[15] E. Galembeck, A. Alonso, N.C. Meirelles, Effects of polyoxyethylene chain length on erythrocyte hemolysis induced by poly[oxyethylene(*n*)nonylphenol] non-ionic surfactants, Chem.-Biol. Interact. 113 (1998) 91–103.
[16] A. Miseta, P. Bogner, A. Szarka, M. Kellermayer, C. Galambos, D.N. Wheatley, I.L. Cameron, Effect of non-lytic concentrations of Brij series detergents on the metabolism-independent ion permeability properties of human erythrocytes, Biophys. J. 69 (1995) 2563–2568.
[17] H. Heerklotz, H. Binder, G. Lantzsch, G. Klose, Membrane/water partition of oligo(ethylene oxide) dodecyl ethers and its relevance for solubilization, Biochim. Biophys. Acta 1196 (1994) 114–122.
[18] H. Heerklotz, J. Seelig, Correlation of membrane/water partition coefficients of detergents with the critical micelle concentration, Biophys. J. 78 (2000) 2435–2440.
[19] J.S. Binford, W.H. Palm, Absorption of surfactants by membranes: erythrocytes versus synthetic vesicles, Biophys. J. 66 (1994) 2024–2028.
[20] P. Preté, K. Gomes, S. Malheiros, N. Meirelles, E. de Paula, E. Solubilization of human erythrocyte membranes by non-ionic surfactants of the polyoxyethylene alkyl ethers series, Biophys. Chemist. 97 (2002) 45–54.
[21] E. Pantaler, D. Kamp, C. Haest, Acceleration of phospholipid flip-flop in the erythrocyte membrane by detergents differing in polar headgroup and alkyl chain length, Biochim. Biophys. Acta 1509 (2000) 397–408.
[22] H.J. Deuling, W. Helfrich, The curvature elasticity of fluid membranes, J. Phys. (France) 37 (1976) 1335–1345.
[23] W. Helfrich, Blocked lipid exchange in bilayers and its possible influence on the shape of vesicles, Z. Naturforsch., C 29 (1974) 510–515.
[24] E. Evans, R. Skalak, Mechanics and Thermodynamics of Biomembranes, CRC Press, Boca Raton, FL, 1980.
[25] A. Iglič, V. Kralj-Iglič, B. Božič, M. Bobrowska-Hägerstrand, B. Isomaa, H. Hägerstrand, Torocyte shapes of red blood cell daughter vesicles, Bioelectrochemistry 52 (2000) 203–211.
[26] M. Fošnarič, M. Nemec, V. Kralj-Iglič, H. Hägerstrand, M. Schara, A. Iglič, Possible role of anisotropic membrane inclusions in stability of torocyte red cell daughter vesicles, Colloids Surf., B Biointerfaces 26 (2002) 243–253.
[27] K. Bohinc, V. Kralj-Iglič, S. May, Interaction between two cylindrical inclusions in a symmetric lipid bilayer, J. Chem. Phys. 119 (2003) 7435–7444.
[28] J. Israelachvili, H. Wennerström, Role of hydration and water structure in biological and colloidal interactions, Nature 379 (1996) 219–225.
[29] J.N. Israelachvili, Intermolecular and Surface Forces, 2nd ed., Academic Press, London, 1992.
[30] B. Samuel, N. Mohandas, T. Harrison, H. McManus, W. Rosse, M. Reid, K. Haldar, The role of cholesterol and glycosylphosphatidylinositol-anchored proteins of erythrocyte rafts in regulating raft protein content and malarial infection, J. Biol. Chem. 276 (2001) 29319–29329.
[31] V. Kralj-Iglič, S. Svetina, B. Žekš, Shapes of bilayer vesicles with membrane embedded molecules, Eur. Biophys. J. 24 (1996) 311–321.
[32] V. Kralj-Iglič, V. Heinrich, S. Svetina, B. Žekš, Free energy of closed membrane with anisotropic inclusions, Eur. Phys. J., B Cond. Matter Phys. 10 (1999) 5–8.
[33] M. Fošnarič, V. Kralj-Iglič, K. Bohinc, A. Iglič, S. May, Stabilization of pores in lipid bilayers by anisotropic inclusions, J. Phys. Chem., B 107 (2003) 12519–12526.
[34] H. Sprong, P. van der Sluijs, G. van Meer, How proteins move lipids and lipids move proteins, Nat. Rev., Mol. Cell Biol. 2 (2001) 504–512.
[35] V. Kralj-Iglič, A. Iglič, H. Hägerstrand, P. Peterlin, Stable tubular microexovesicles of the erythrocyte membrane induced by dimeric amphiphiles, Phys. Rev., E 61 (2000) 4230–4234.
[36] H. Hägerstrand, J. Bobacka, M. Bobrowska-Hägerstrand, V. Kralj-Iglič, M. Fošnarič, A. Iglič, Oxyethylene chain–cation complexation; nonionic polyoxyethylene detergents may attain a positive charge and demonstrate electrostatic head group interactions, Cell. Mol. Biol. Lett. 6 (2001) 161–165.
[37] N.N. Markuzina, S.B. Mokrov, O.K. Stefanova, S.N. Sementsov, Yo.M. Volkov, E.A. Ranieva, Electrode properties of film membranes containing alkoxylated alkylophenols as nonionic surfactants, Russ. J. Appl. Chem. 66 (1993) 1765–1769.
[38] M. Rosen, X. Hua, Surface concentrations and molecular interactions in binary mixtures of surfactants, J. Colloid Interface Sci. 86 (1982) 164–172.
[39] M. Rosen, T. Gao, Y. Nakatsuji, A. Masuyama, Synergism in binary mixtures of surfactants. Mixtures containing surfactants with two hydrophilic and two or three hydrophobic groups, Colloids Surf., A Physicochem. Eng. Asp. 88 (1994) 1–11.
[40] E. Malinowska, A. Manzoni, M.E. Meyerhoff, Potentiometric response of magnesium-selective membrane electrode in the presence of nonionic surfactants, Anal. Chim. Acta 382 (1999) 265–275.
[41] E. Malinowska, M.E. Meyerhoff, Influence of nonionic surfactants on the potentiometric response of ion-selective polymeric membrane electrodes designed for blood electrolyte measurements, Anal. Chem. 70 (1998) 1477–1488.
[42] P. Liljekvist, B. Kronberg, Comparing decyl-beta-maltoside and octaethyleneglycol mono *n*-decyl ether in mixed micelles with dodecyl benzenesulfonate: 1. Formation of micelles, J. Colloid Interface Sci. 222 (2000) 159–164.
[43] Y. Sakai, K. Ono, T. Hidaka, M. Takagi, R.W. Cattrall, Extraction of alkali metal ions and tetraalkylammonium ions with ionic surfactants containing a polyoxyethylene chain, Bull. Chem. Soc. 73 (2000) 1165–1169.
[44] S. Schwarz, C. Haest, B. Deuticke, Extensive electroporation abolishes experimentally induced shape transformations of erythrocytes: a consequence of phospholipid symmetrization? Biochim. Biophys. Acta 1421 (1999) 361–379.
[45] M. Le Maire, J.V. Moller, P. Champeil, Binding of a nonionic detergent to membranes: Flip-flop rate and location on the bilayer, Biochemistry 26 (1987) 4803–4810.
[46] B. Isomaa, H. Hägerstrand, G. Paatero, Shape transformations induced by amphiphiles in erythrocytes, Biochim. Biophys. Acta 899 (1987) 93–103.
[47] M. Le Maire, P. Champeil, J.V. Moller, Interaction of membrane proteins and lipids with solubilizing detergents, Biochim. Biophys. Acta 1508 (2000) 86–111.
[48] S.L. Schrier, A. Zachowski, P.F. Devaux, Mechanisms of amphipath-induced stomatocytosis in human erythrocytes, Blood 79 (1992) 782–786.
[49] J.B. Fournier, Nontopological saddle-splay and curvature instabilities from anisotropic membrane inclusions, Phys. Rev. Lett. 76 (1996) 4436–4439.